Journal of Sol-Gel Science and Technology 28, 81–86, 2003

Hybrid Sol-Gel Coatings Produced from TEOS and γ-MPS

S. PELLICE AND PABLO GALLIANO
INTEMA-Conicet. Mar del Plata, Argentina

Y. CASTRO AND A. DURÁN*
Instituto de Cerámica y Vidrio (CSIC), Campus de UAM, Cantoblanco, Madrid, Spain
aduran@icv.csic.es

Received September 19, 2002; Accepted March 18, 2003

Abstract. Hybrids sols from tetraetoxysilane (TEOS) and 3-(methacryloxypropyl) trimethoxysilane (γ-MPS) were prepared in acid medium for different TEOS/γ-MPS ratios and were modified by the addition of a colloidal silica suspension. The stability of the different sols was evaluated by viscosity measurements; the sols showed a Newtonian behaviour and the ageing effect was negligible even after two months from their preparation. Coatings were obtained by dipping at different withdrawal rates and heat-treated between 150 and 250°C. Transparent coatings with thickness higher than 4 μm were reached for most of the studied compositions. The surface microhardness of coatings for each composition and thermal treatment was evaluated by the pencil hardness test. The thermal stability was followed by simultaneous thermogravimetric and differential thermal analysis (TGA-DTA) determining the limit temperatures at which the coatings can be treated without losing its hybrid character. A structural analysis was made by deconvolution of Fourier transformed infrared spectra (FTIR) of self-supported films observing the influence of the organic groups on the silica network.

Keywords: sol-gel, hybrid coatings, γ-MPS, structure, microhardness

Introduction

Sol-gel method is a simple technique used to produce adherent and crack-free silica coatings, whose most important feature consists on the low sintering temperatures [1, 2]. In the last years, hybrid organic-inorganic coatings have been developed in order to improve mechanical, optical and abrasion properties [3–5]. Trifunctional alkoxysilanes $R'Si(OR)_3$, where R and R′ are alkyl groups, have been used as starting materials to introduce organic groups in the coatings. Reactive organic groups present in the alkyl chains, such as vinyl and methacryl groups, can react at low temperature producing crosslinked polymeric networks. One of the trialkoxysilanes usually employed for this purpose is the 3-(methacryloxypropyl)trimethoxisilane (γ-MPS). Recently, hybrid coatings and bulk materials have been obtained from the hydrolysis and condensation of γ-MPS, the microhardness of these coatings being lower than that of glass slides [6].

The silica porosity and Si—O—Si bond stresses were related to the longitudinal optical (LO) and transversal optical (TO) mode peaks in FTIR spectra [7–10]. In this sense, the effect of the organic content on the silica porosity and Si—O—Si bond tensile strain have a high importance on the coating properties, such as critical thickness and scratch resistance.

The aim of this work was to obtain hybrid inorganic-organic coatings from TEOS and γ-MPS, modified by adding different molar ratios of a colloidal silica suspension in order to increase their hardness and scratch resistance.

*To whom all correspondence should be addressed.

Experimental

Two series of solutions were prepared. The series S (S1–S4) was obtained from tetraethoxysilane (TEOS) and 3-(methacryloxypropyl)trimethoxysilane (γ-MPS) by adding diluted HNO_3 (0.1 N) to produce hydrolysis and condensation reactions. TEOS/γ-MPS molar ratio was varied from 90/10 to 25/75 and the molar ratios H_2O/(TEOS + γ-MPS) were changed between 3.25–3.9. Initial sols were diluted with absolute ethanol up to a concentration (expressed as SiO_2) of 150 g/l.

The other series of solutions C (C1–C3) was prepared mixing TEOS, γ-MPS and a colloidal suspension of silica (Levasil 200S, Bayer, Germany, particle size 15 nm, and pH 9). Concentrated HNO_3 was used as catalyst to reach a pH between 2–3. The molar ratio TEOS/γ-MPS was equal to 1, and (TEOS + γ-MPS)/$SiO_{2\,\text{colloidal}}$ molar ratio varied between 60/40 and 30/70. A final silica concentration of 250 g/l was obtained by diluting with a mixture of isopropyl/butyl glycol.

Table 1 shows the molar ratios of TEOS, γ-MPS, and the colloidal silica for each studied solutions.

The stability of the sols was evaluated through viscosity evolution, using a rheometer (Haake, RS50, Germany) under controlled rate conditions at 25°C.

Thermo Gravimetric Analysis (TGA) and Differential Thermal Analysis (DTA) were performed on bulk specimens gelled at 60°C from series S. These analyses were carried out at a heating rate of 10°C/min up to 500°C in air, using a Netzsch (Simultaneous Thermal Analysis STA 409) equipment. Self-supported layers of series S were produced by gelling at 60°C and tested by TGA using the same conditions. Isothermal TGA was also performed to simulate curing conditions, at two temperatures, 150 and 250°C for 1 hour.

Table 1. Compositions of the sols in mol%.

	mol%		
Compositions	TEOS	γ-MPS	Colloidal SiO_2
S1	90	10	
S2	75	25	
S3	50	50	
S4	25	75	
C1	30	30	40
C2	20	20	60
C3	15	15	70

Fourier Transformed Infrared Spectroscopy (FTIR, Mattson Genesis II) in transmittance mode was performed on self-supported films of the series S. The spectra in the region between 1300 and 950 cm^{-1} were deconvoluted to follow the evolution of the LO and TO Si—O—Si peaks around 1130 and 1060 cm^{-1} using Peakfit software.

Coatings were obtained on glass slides by dip-coating at a withdrawal rate between 10 and 52 cm/min to determine the critical thickness corresponding to each sol. The films were dried at room temperature and densified during 30 minutes at temperatures between 100°C and 300°C with a heating rate of 10°C/min in air. The thickness of the coatings was measured by profilometry (Talystep, UK) and their surface microhardness was determined by the Pencil Hardness Test Method (Braive Instruments, Belgium) [11].

Results and Discussion

The sols were characterised by determining viscosity changes with the ageing time. All the sols showed a Newtonian behaviour, maintained for at least nine weeks (1500 hours) without significant changes. When nanoparticles are added to the sol, the stability is still high although the viscosity slightly increases from 3.5 mPa · s for the series S to 5 mPa · s for series C. Figure 1 shows the evolution of the viscosity with the shear rate for the sols S3 and C3. As observed, the viscosity of sol C3 remains Newtonian and low, in spite of its high concentration (250 g/l with a ratio 70/30 between $SiO_{2\,\text{colloidal}}/SiO_2$).

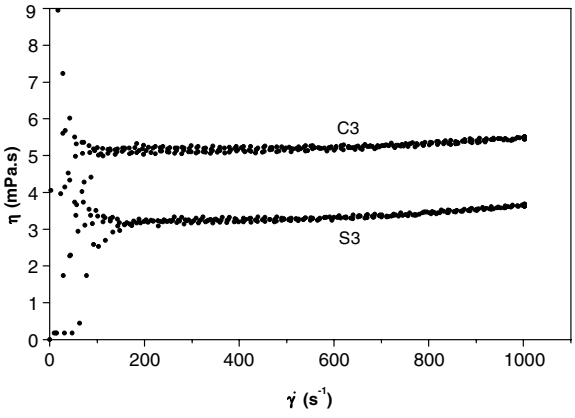

Figure 1. Rheological curves showing the raise of viscosity with the addition of colloidal silica.

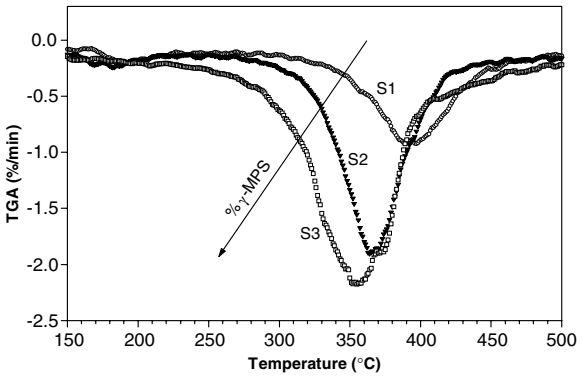

Figure 2. TGA curves as a function of temperature.

Figure 2 presents the thermo gravimetric curves of films gelled at 60°C, showing that the higher the organic concentration in the samples the higher is the degradation rate.

TGA and DTA tests were also performed with bulk gelled samples using the same test parameters. The results show a similar trend, although the temperatures of degradation of organic groups take place at lower temperatures, probably due to the lower porosity exhibited for the films compared with these obtained for the bulk samples. The rate of degradation is faster with increasing porosity due to greater oxygen diffusion. Thus, gas diffusion and oxidation of the organic species in the bulk porous material is favoured.

On the other hand, isothermal TGA at 150 and 250°C were performed on self-supported gelled films from series S, Fig. 3. The first part of the curves of the Fig. 3(a) corresponds to water and alcohol losses. Since the hydrophobic character of the material increases with increasing γ-MPS content these mass loss is lower for higher organic contents. At 150°C only S3 layers showed some degradation with time. On the other hand, in the test performed at 250°C, Fig. 3(b), two different sections are observed. The first corresponds also to water and alcohol loss, and the second is originated by thermal degradation of the organic species present in the γ-MPS. At this temperature S1 and S2 suffer only slight degradation, compared with the higher rate of S3 layers.

Coatings onto glass slides were prepared at different withdrawal rates and cured between 100 and 300°C. Coatings obtained from sol S3, thermally treated at 150°C, C1 and C2 thermally treated at 250°C, and S4 at every thermal treatment temperature, exhibit lack of homogeneity seen as waves or drips. These dripping phenomena may be caused by the presence of γ-MPS as reagent. When the organic fraction is higher than 40% drying at room temperature is not totally effective. When samples are subjected to thermal treatments, the film viscosity reduces and the film flows producing the dripping phenomenon. In order to avoid this behaviour, a pre-curing step at lower temperature and/or the addition of a curing agent to avoid plastic flow is suggested.

The critical thickness, defined as the maximum thickness without cracks, decreases with increasing densification temperature. Figure 4 shows the evolution of the critical thickness for S compositions as a function of densification temperature. Critical thickness shows a large rise when the organic content increases or the temperature of thermal treatment decreases. Data points signed with ascendant arrows, indicate that

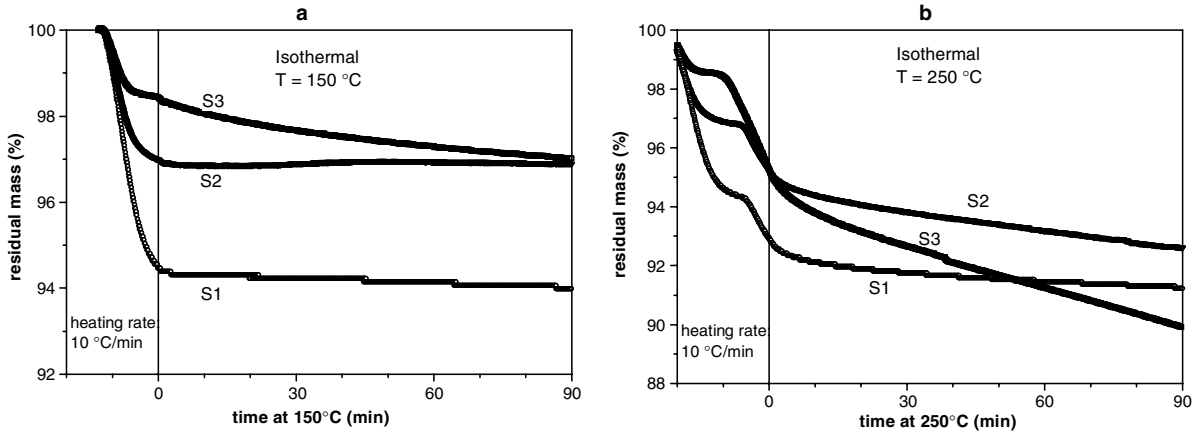

Figure 3. Isothermal TGA curves for: (a) 150°C and (b) 250°C as a function of time for series S.

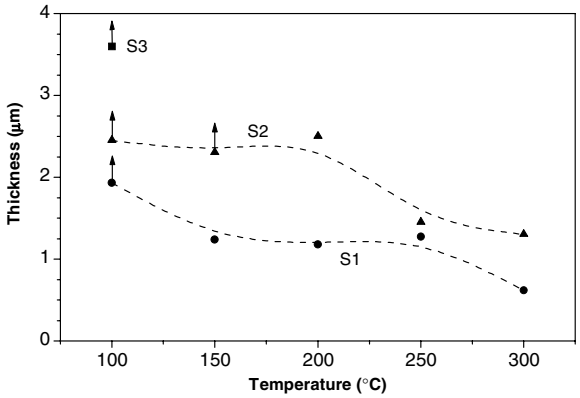

Figure 4. Maximum and critical thickness as a function of densification temperature for series S.

no critical thickness was reached, this thickness corresponding to the maximum withdrawal rate used in this work. In case of series C no cracks were produced under any experimental condition, similar to the S3 composition, although thickness was not measured because of the dipping phenomenon.

From TGA-DTA results and coating evolution with curing heat treatment, the limit temperature can be deduced to avoid degradation and lack of homogeneity in the coatings. Thus, curing temperature should be lower than 250°C for S1, 200°C for S2 and 150°C for S3 and series C.

Since $\mathbf{e} \alpha \mathbf{v}^n$, where **e** is the coating thickness in μm, and **v** is the withdrawal rate in cm/min; n was calculated by least-squares regression. The values obtained vary between 0.79 and 0.87 for each composition and thermal treatment, while the deduced value by Strawbridge et al. [12] and Guglielmi et al. [13] for inorganic coatings is 0.5. Deviations in this slope are attributed to the rheological and flowing behaviour of the sols and the singular hybrid structure of coatings obtained from γ-MPS, although this effect must be further studied for total clarification.

An analysis by FTIR was made on S series and pure silica films. The deconvolution of FTIR spectra in the region between 1300 and 950 cm^{-1}, allows study of the evolution of the bonds corresponding to TO mode of Si─O─Si vibration ($\sim$1060 cm^{-1}) and the LO mode around 1130 cm^{-1} (Fig. 5). The area in the frame in

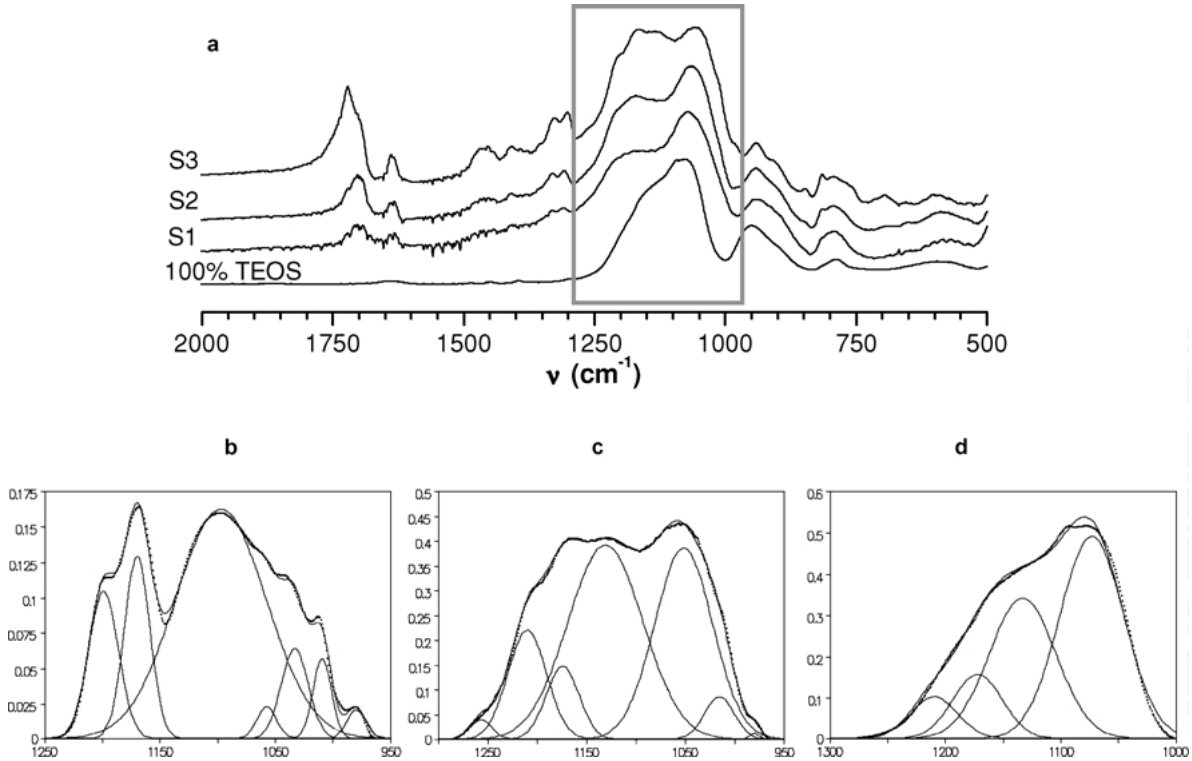

Figure 5. FTIR spectra for (a) the S series and spectra of the pure γ-MPS and deconvoluted spectra for pure γ-MPS (b), TEOS/γ-MPS 50/50 (c), and pure silica (d) films.

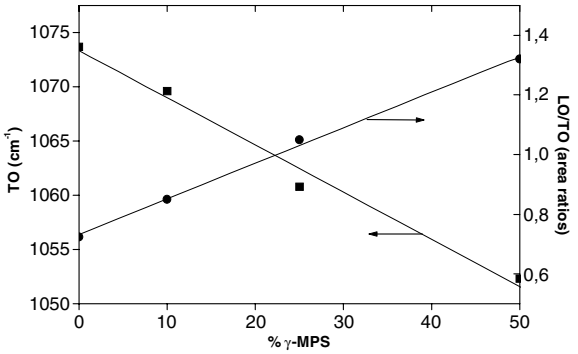

Figure 6. TO shifting and LO/TO area ratio as a function of γ-MPS content.

Fig. 5(a), indicates the selected region, that is deconvoluted in Fig. 5(b)–(d), for pure γ-MPS, TEOS/γ-MPS 50/50, and pure silica films respectively.

The analysis of the shifting of TO frequency and the ratio of the LO and TO peak areas, Fig. 6, leads to two important observations about the effect of the organic material on the coating structure. A significant decrease in the frequency of the TO peak is observed for increasing γ-MPS content, this indicating a less straining of the Si—O—Si bonds. On the other hand, the ratio LO/TO, calculated from the areas of these bands, increases with γ-MPS content. Since LO mode has been related with the porosity of the coating [8, 9], this suggests that the addition of the organic leads to a more porous structure. This agrees with TGA and microhardness results and explains the strong increase in the critical thickness of the coatings with the addition of γ-MPS to the starting composition.

The effect of the thermal treatment and composition of the coatings was evaluated through microhardness by the Pencil Hardness test. Since the harder pencil available is 9H, the points marked with an arrow (↑) in Fig. 7 indicate that these coatings show a hardness >9H. The pencil hardness of an Epoxy Powder coating is 5H (30.2 Knoop Hardness Number) [14], considerably lower than the hybrid coatings here analysed.

Two different failure modes were observed, a scratching mode in which the lines may be closed when pressure ceases, and a tearing mode that involves loss of material. The results show, Fig. 7(a), that an increase in the densification temperature produces a small reduction of the scratch resistance and an increase in the tear resistance, this being probably due to the loss of hybrid character of the coating with temperature. On the other hand, Fig. 7(b), an important drop in the scratch resistance was observed for the S3 coating with respect to S1 and S2 treated at 150°C, along with an increase in the tear resistance. Figure 7(c) shows the effect of inorganic particles on microhardness. C1 and C2 can be compared with S3, since they have the same TEOS/γ-MPS ratio, showing an increase in the scratching resistance. C3 with a ratio (TEOS + γ-MPS)/$SiO_{2\,colloidal} = 30/70$ presents the same scratching but lower tearing behaviours, probably due to an excessive particle content.

As general conclusion, the higher the inorganic content, the higher is the microhardness of the coating. Indeed, tear resistance higher than 8H was obtained for all the coating compositions and treatments, these being much harder than polymeric coatings reported above.

Conclusions

Hybrid silica sols prepared from TEOS and γ-MPS show a Newtonian behaviour, ageing effect being negligible even after two months of storage.

The limit temperature for coating densification decreases with γ-MPS content, and it should be always

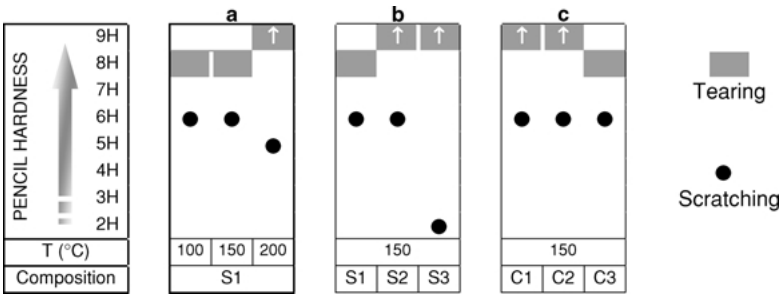

Figure 7. Microhardness (Pencil Test) of coatings of series S and C.

lower than 250°C for S1 sol and 200°C and 150°C for S2 and S3 sols respectively.

The addition of γ-MPS leads to a strong increase in the coating critical thickness, related to the higher porosity and stress relaxation induced in the silica structure. Furthermore, the value of n (the parameter relating the coating thickness with the withdrawal rate) strongly increases from 0.5 (in non-containing γ-MPS sols) to 0.79–0.87, depending on γ-MPS content.

The increment of porosity and the stress relaxation evidenced by the FTIR results explains the strong increase in the critical thickness of the coatings with the addition of γ-MPS to the starting alkoxides.

Two kinds of pencil microhardness were observed, scratch and tear modes. A decrease in the scratch resistance was observed with increasing γ-MPS content and densification temperature. On the other hand, the addition of colloidal silica improves the scratch resistance for high γ-MPS content (50%). Tear resistance higher than 8H were obtained for all the coatings compositions and treatments, these being much harder than reported sol-gel polymeric coatings.

Acknowledgments

This work has been partially financed by project MAT2000-0952-C02-01 and the Programme CYTED (AECI) through the Network VIII-E and the Project VIII.9.

References

1. C.J. Brinker and G.W. Scherer, in *Sol-Gel Science: The Physics and Chemistry of Sol-Gel Processing*, edited by Harcourt Brace Jovanovich (Academic Press, Inc., Boston, 1990).
2. C.J. Brinker, A.J. Hurd, and P.R. Shunrk, J. Non-Cryst. Solids **147**, 424 (1992).
3. H. Schmidt, G. Rinw, R. Nab, and D. Spor, Mat. Res. Soc. Symp. Proc. **121**, 743 (1988).
4. D.R. Uhlmann, G. Teowee, and J. Boulton, J. Sol-Gel Sci. Technol. **8**, 17 (1997).
5. G. With, R.H. Brzesowsky, J.G. van Lierop, and I.J.M. Snijkers-Hendrickx, J. Non-Cryst. Solids **226**, 105 (1998).
6. M.A. Fanovich, S.A. Pellice, P.G. Galliano, and R.J.J. Williams, J. Sol-Gel Sci. Technol. **23**, 45 (2002).
7. J. Gallardo, P. Galliano, and A. Durán, J. Sol-Gel Sci. Technol. **19**, 393 (2000).
8. J. Gallardo, A. Durán, D. Di Martino, and R.M. Almeida, J. Non-Cryst. Solids **298**, 219 (2002).
9. J. Gallardo, P. Galliano, and A. Durán, Soc. Esp. Cerám. Vidrio. **40**(1), 31 (2001).
10. A. Fidalgo and L.M. Ilharco, J. Non-Cryst. Solids **283**, 144 (2001).
11. ASTM D 3363—92[a]. Standard Test Method for Film Hardness by Pencil Test.
12. I. Strawbridge and P.F. James, J. Non-Cryst. Solids **86**, 381 (1986).
13. M. Guglielmi and S. Zenezini, J. Non-Cryst. Solids **121**, 303 (1990).
14. P.R. Guevin, J. Coatings Technol. **67**, 840 (1995).